Single-particle states in ^{151}Tm and ^{151}Er: Systematics of neutron states in $N=83$ nuclei

Y. A. Akovali and K. S. Toth
Oak Ridge National Laboratory, Oak Ridge, Tennessee 37831

A. L. Goodman
Tulane University, New Orleans, Louisana 70118

J. M. Nitschke, P. A. Wilmarth, and D. M. Moltz
Lawrence Berkeley Laboratory, Berkeley, California 94720

M. N. Rao
Universidade de São Paulo, Caixa Postal 20516, São Paulo, Brazil 01498

D. C. Sousa
Eastern Kentucky University, Richmond, Kentucky 40475
(Received 25 July 1988)

With the use of mass-separated sources, the β-decay properties of ^{151}Yb and ^{151}Tm were investigated. The $h_{11/2}$, $s_{1/2}$, $d_{3/2}$, $d_{5/2}$, and $g_{7/2}$ single-proton states in ^{151}Tm and the $f_{7/2}$, $h_{9/2}$, $p_{3/2}$, $i_{13/2}$, and probably the $p_{1/2}$ single-neutron states in ^{151}Er were identified. Systematics of neutron states in even-Z $N=83$ isotones are compared with predictions of spherical Hartree-Fock-Bogoliubov calculations.

I. INTRODUCTION

We recently reported[1] on the β decay of ^{149}Er and the isomeric decay of ^{149}Er^m to low-lying levels in ^{149}Ho and ^{149}Er, respectively. This allowed us to extend the systematics of single-proton states in $N=82$ odd-Z nuclei to $Z=67$ and of single-neutron states in $N=81$ even-Z nuclei to $Z=68$. Spherical Hartree-Fock-Bogoliubov (HFB) calculations were made[1] and compared with these experimental systematics. It was found that the theoretical trends for the proton levels agreed with experiment while those for the neutron-hole levels did not. In particular, the calculations did not account for the constant excitation energy of the $h_{11/2}$ neutron level in $N=81$ nuclei with $Z \geq 58$.

The present paper describes a study of ^{151}Yb decay (designed to supplement our ^{149}Er results), and of the β decays of the high- and low-spin ^{151}Tm isomers to levels in the $N=83$ nucleus ^{151}Er. Experimental systematics for neutron states in even-Z $N=83$ isotones are brought up to date. They are then compared with predictions from HFB calculations.

Isotopes with $A=151$ were produced by bombarding a 1.5-mg/cm^2-thick N_2 gas-cooled[2] target of ruthenium, enriched in ^{96}Ru to 96.5% and deposited onto a 2.0-mg/cm^2-thick HAVAR foil, with ^{58}Ni ions from the Lawrence Berkeley Laboratory SuperHILAC. After traversing the N_2 gas-cooled target-cell window and the HAVAR backing the 360-MeV-^{58}Ni beam had a calculated energy of 250 MeV at the center of the target.

Reaction products with $A=151$ were mass separated with the OASIS separator[3] on-line at the SuperHILAC and transported ion optically to a shielded area. There they were implanted in a 50-μm-thick Mylar tape for a period of 4 s and then transported to a counting station for assay with a Si particle telescope, a thin plastic scintillator, a planar hyperpure Ge detector, and two n-type Ge detectors with relative efficiencies of 24% and 52%. With this detector arrangement (a schematic drawing of the setup can be seen in Fig. 1 of Ref. 4) coincidences between particles, photons, and positrons were recorded in an event-by-event mode. Events in all detectors were tagged with a time signal from a quartz controlled clock for half-life determinations. Singles γ-ray data were also taken with the 24% γ-ray detector in a multispectrum mode for additional half-life information. A new source of $A=151$ isotopes was provided by the computer controlled tape system at the conclusion of each 4-s counting cycle.

II. RESULTS

A. General

The incident energy was selected to optimize the production of ^{151}Yb and ^{151}Tm; their cross sections at 250 MeV are predicted[5] to be 8 and 60 mb, respectively. Mass=151 nuclides with $Z>70$, due to a reduced probability for neutron evaporation, have very small yields; e.g., the cross section calculated[5] for ^{151}Lu is 50μb. On the other hand, nuclides with $Z<69$ could be produced only in reactions involving ruthenium isotopes with $A \geq 98$ (less than 3.5% of the target material). Thus, ^{151}Er and ^{151}Ho seen in our experiment resulted mainly from ^{151}Tm decay.

Figures 1 and 2 show portions of the singles γ-ray

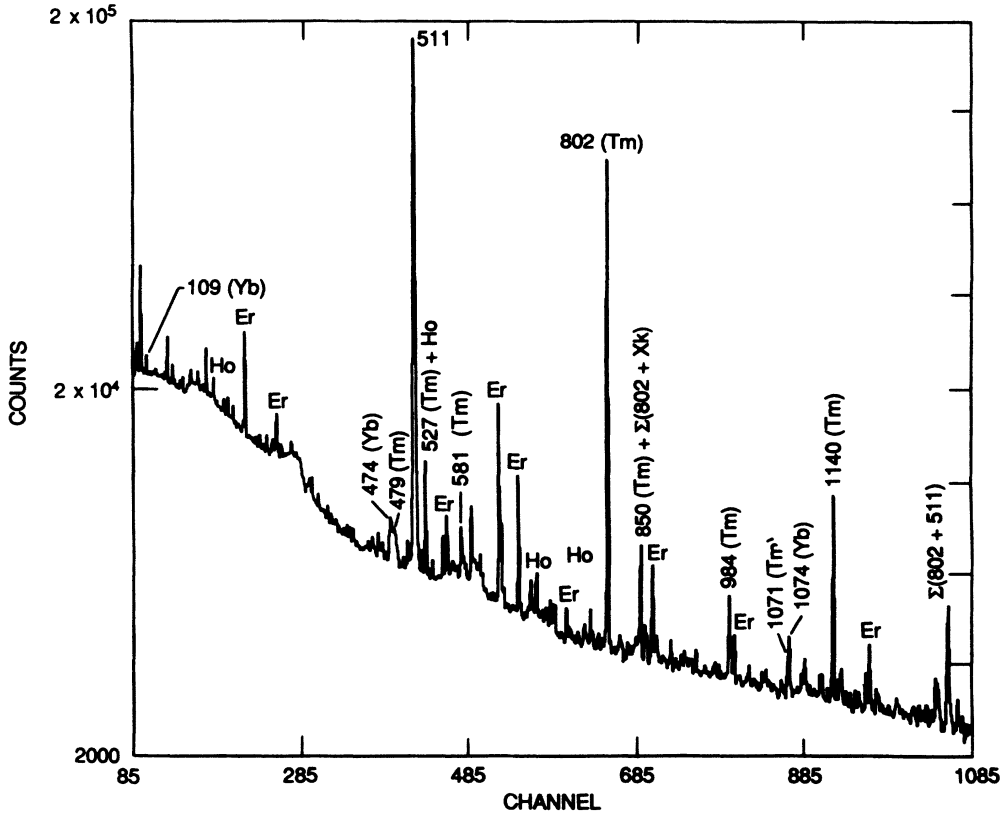

FIG. 1. Portion (100–1350 keV) of the singles $A=151$ γ-ray spectrum measured during 4-s counting intervals following ^{58}Ni bombardments of ^{96}Ru. Only selected γ rays are labeled by energy and element.

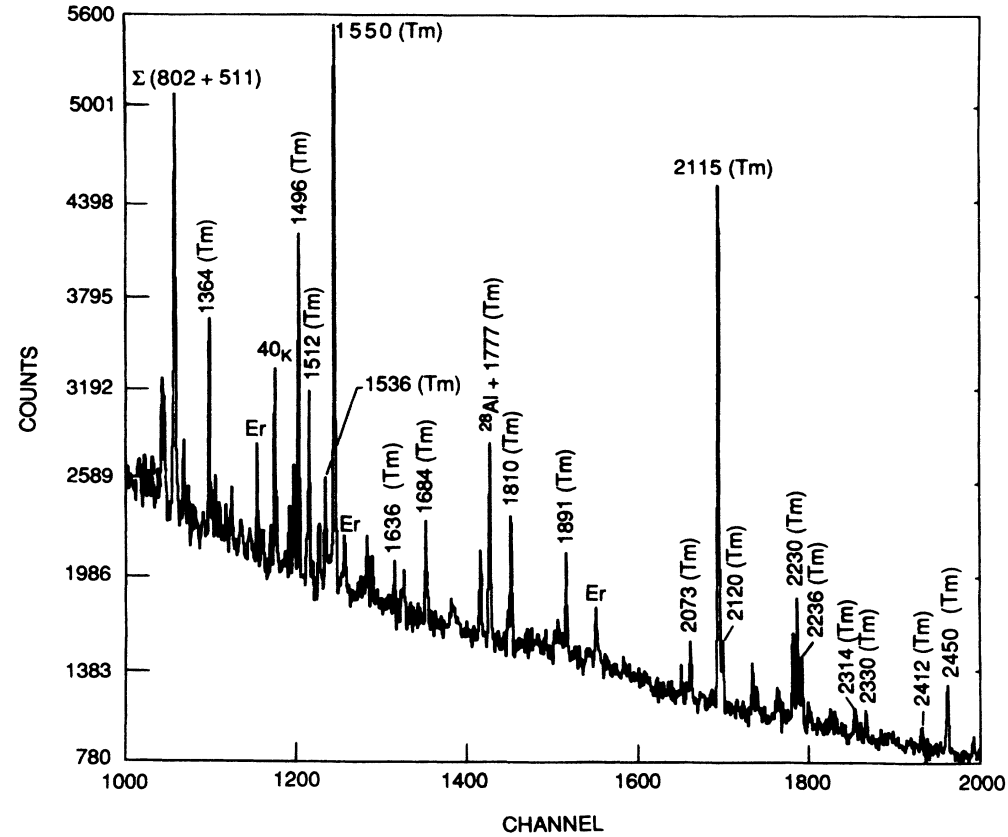

FIG. 2. Portion (1250-2500 keV) of the singles $A=151$ γ-ray spectrum measured during 4-s counting intervals following ^{58}Ni bombardments of ^{96}Ru. Only selected γ rays are labeled by energy and element.

spectra accumulated during the 4-*s* counting intervals. For clarity only strong γ-ray peaks are labeled by energy and element. Assignments are based on coincidences with K x rays and other γ rays, and on half-life measurements. As expected from the predicted cross sections, ^{151}Tm γ rays are much more intense than those of ^{151}Yb. Also, in accord with the cross-section calculations, there was no evidence in our particle, x-ray, and γ-ray spectra for the presence of isotopes with $Z>70$; however, yields for these short-lived (the ^{151}Lu $T_{1/2}$ is 90 ms) isotopes would also be suppressed in our experiment because of the 4-s tape cycle, the 160-ms tape transport time, and the holdup in the separator ion source.

A large number of transitions were found to follow the β decay of 23-s ^{151}Er which was first identified[6] from an observed growth period in the decay curve of the ^{151}Ho low-spin α-particle group. Subsequently, two γ-ray transitions that follow ^{151}Er decay were reported[7] and, more recently, a partial decay scheme has been presented.[8] We concentrate in this work on single-proton states in $N=82$ and single-neutron states in $N=83$ nuclei, and no attempt was made to complete the ^{151}Er decay scheme.

B. Single-proton states in $^{151}_{69}Tm_{82}$

The isotope ^{151}Yb was first identified[9,10] by its β-delayed proton emission. In Ref. 10 it was established that, as is the case for other even-Z $N=81$ isotones,[1] there is in ^{151}Yb an $s_{1/2}$ ground state and an $h_{11/2}$ isomer. Within error limits the two levels were determined to have the same 1.6-s half life.[10] Kleinheinz *et al.*,[11] who investigated γ rays following ^{151}Yb β decay, reported half-lives that agreed with the values of Ref. 10 and observed three transitions in cascade with each other. They proposed[11] that the γ rays deexcited the $g_{7/2}\rightarrow d_{5/2}\rightarrow d_{3/2}\rightarrow s_{1/2}$ single-proton levels in ^{151}Tm.

We also observed these three γ rays, i.e., 108.5, 474.2, and 520.8 keV. They are seen in Fig. 1 and in Fig. 3(a) where we show the spectrum in coincidence with Tm $K\alpha_1$ x rays. The fact that they are in cascade is illustrated in Fig. 4 where the 474.2- and 520.8-keV transitions are seen to be in coincidence with the 108.5-keV γ ray. In addition, we assign two new γ rays, 568.8 and 1074.0 keV, to the decay of ^{151}Yb. Table I summarizes energies and relative intensities for ^{151}Yb γ-ray transitions and compares their intensities with the values reported by Kleinheinz *et al.*[11]

According to the shell model, the ^{151}Yb ground state has three proton pairs coupled to 0^+ in the $h_{11/2}$ shell above the $Z=64$ closure and one neutron in the $s_{1/2}$ shell just below $N=82$; the $h_{11/2}$ and $d_{3/2}$ neutron orbitals are filled. A large part of the beta-decay-strength is expected to go to the $(\pi s_{1/2}^{-1})$ state following the $\pi s_{1/2}\rightarrow\nu s_{1/2}$ transition, and to higher energy levels with $(\pi h_{11/2}, \nu h_{9/2}, \nu s_{1/2})$ configurations following the $\pi h_{11/2}\rightarrow\nu h_{9/2}$ transition from one of the paired protons in the $h_{11/2}$

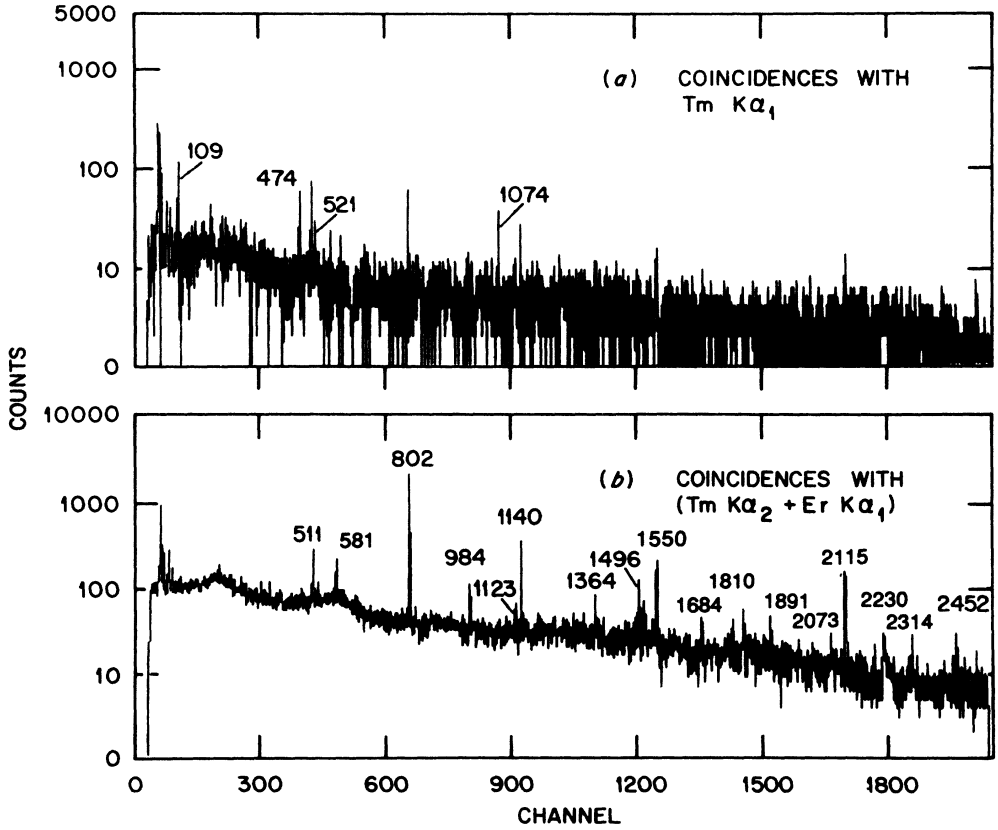

FIG. 3. Gamma rays observed in coincidence with Tm $K\alpha_1$ [part (a)] and with (Er $K\alpha_1$ + Tm $K\alpha_2$) [part (b)] x rays for $A=151$ nuclides.

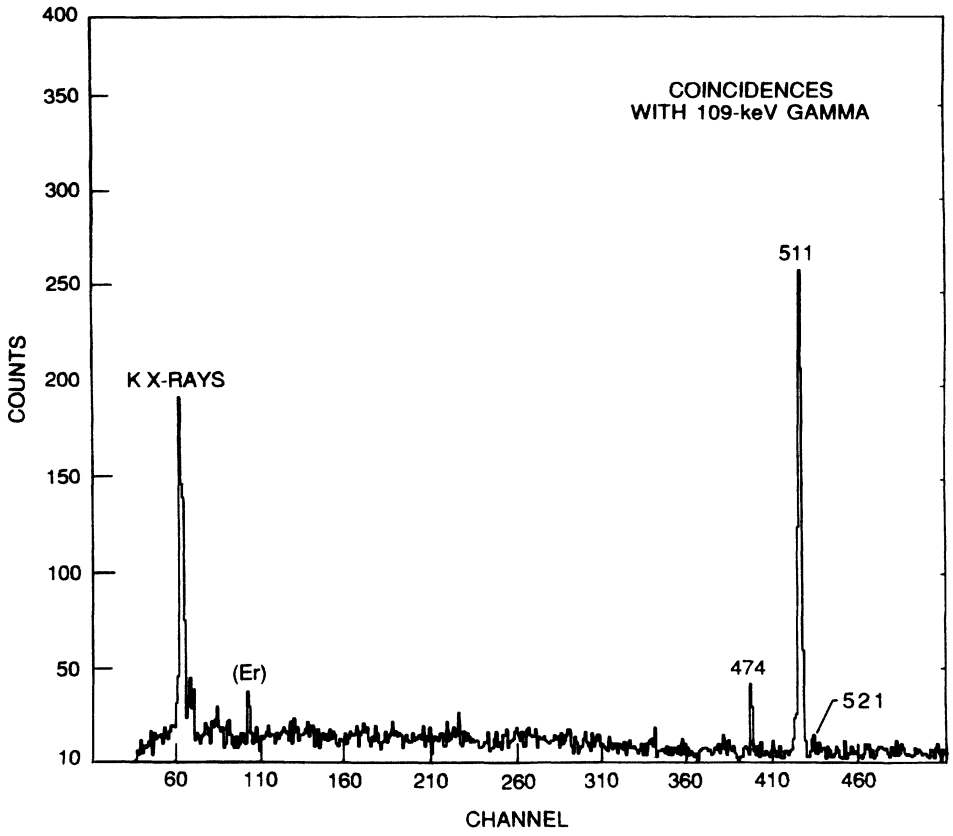

FIG. 4. Gamma rays observed in coincidence with the 108.5-keV transition that follows ^{151}Yb decay.

state. Other high-lying levels could receive some direct feeding through the $\pi d_{5/2} \rightarrow \nu f_{5/2}$, $\nu f_{7/2}$, $\nu p_{3/2}$; $\pi g_{7/2} \rightarrow \nu f_{5/2}$, $\nu f_{7/2}$, $\nu h_{9/2}$; or $\pi h_{11/2} \rightarrow \nu i_{13/2}$ first-forbidden transitions.

The ^{151}Yb isomeric state, based on systematics of orbitals in $N=81$ isotones, has one hole in the $h_{11/2}$ neutron orbital while the $d_{3/2}$ and $s_{1/2}$ orbitals are full. The $\pi h_{11/2} \rightarrow \nu h_{11/2}$ transition leading to the $h_{11/2}$ ground state of ^{151}Tm is expected in addition to the β transitions mentioned above (which now populate high-energy states with similar configurations but where the $(\nu h_{11/2}^{-1})$ orbital has replaced the $\nu s_{1/2}$ state).

We did observe weak γ rays possibly in coincidence with the Tm $K\alpha$ x rays that could probably be attributed to the above expected transitions. However, because of the low production yield for ^{151}Yb, their half-lives could not be determined for definite assignments, and for that reason they are not included in Table I. Deexcitation of high-energy levels in ^{151}Tm by γ-ray transitions was therefore not unraveled in this work. Instead, we show a partial decay scheme for ^{151}Yb in Fig. 5 where the β-decay energy of 7.8 MeV is estimated from Q-value systematics given by Wapstra and Audi.[12] The deexcitation of low-spin $(\frac{1}{2}, \frac{3}{2})$ levels at 3.8–5.0 MeV and high-spin $(\frac{9}{2}, \frac{11}{2}, \frac{13}{2})$ levels at 5.0–9.0-MeV excitation energies in ^{151}Tm by proton emission has been discussed in our earlier work.[10]

The lowest available five levels in odd-Z $N=82$ isotones[1,11] are the $g_{7/2}$, $d_{5/2}$, $d_{3/2}$, $s_{1/2}$, and $h_{11/2}$ proton orbitals. Because the three cascading γ rays assigned to

TABLE I. Transitions observed in ^{151}Yb β decay.

E_γ (keV) (This work)	I_γ (relative) (Ref. 11)	Relative intensities (this work) I_γ	$I_\gamma + I_{ce}$
108.5(2)	100	100(5)	351(18)[a]
474.2(4)	192(17)	208(32)	217(33)[a]
520.8(3)	164(16)	156(16)	162(16)[a]
568.1(5)[b]		142(29)	
1074.0(6)		380(38)	380(38)

[a]$M1$ multipolarity assumed.
[b]Not placed in level scheme.

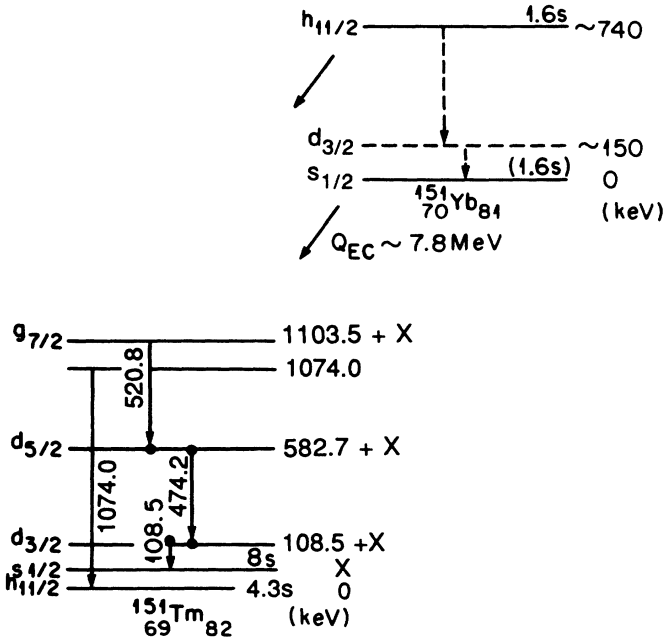

FIG. 5. Partial decay scheme for ^{151}Yb. The excitation energy of the $s_{1/2}$ state in ^{151}Tm (labeled x) is estimated to be ≈ 50 keV (see text).

^{151}Yb β decay are in prompt coincidence they must connect the first four states. Their placement in Fig. 5 is based on their intensities as summarized in Table I. Since crossover transitions were not observed and the deexcited levels have short half-lives the spin sequence is consistent with the monotonic sequence, i.e., $g_{7/2} \rightarrow d_{5/2} \rightarrow d_{3/2} \rightarrow s_{1/2}$, as deduced in Ref. 11. The $g_{7/2}$ and $d_{5/2}$ states are expected to be populated by γ rays from excited states in ^{151}Tm, not by direct beta transitions. Population of the $d_{3/2}$ and $s_{1/2}$ states, on the other hand, should be through direct beta feeding (see Ref. 10 for our β-strength calculations for the $s_{1/2}$ ^{151}Yb ground-state decay), as well as by cascading γ rays from excited states in ^{151}Tm.

In addition, we place the strong 1074.0-keV γ ray deexciting a level at 1074.0 keV. We propose that this state may be populated from the $(\nu h_{11/2}^{-1})$ isomeric state in ^{151}Yb. No strong γ rays, other than Tm K x rays, were discerned in coincidence with the 1074.0-keV γ ray. We measured a half-life of 1.6±0.1 s for the 1074.0-keV γ ray; the decay curve of this γ ray must represent a true measurement of the isomer's half-life in contrast to the decay curves of the Tm $K\alpha$ x rays and of the three cascading γ rays shown in Fig. 5, since these data curves are expected to include contributions from the $s_{1/2}$ ground state. However, there was no indication of a second component in their decay curves. Therefore, as in Ref. 10, we conclude that both the $\frac{1}{2}^-$ ground and the $\frac{11}{2}^-$ isomeric states have, within uncertainties, the same half-life, i.e., 1.6±0.1 s.

Notice in Fig. 5 that the $h_{11/2}$ proton level is indicated as the ^{151}Tm ground state. This placement is based on the fact that while the $s_{1/2}$ level is the ground state in ^{147}Tb (Ref. 13), ^{149}Tb (Ref. 14), and ^{151}Tb (Ref. 15), the $h_{11/2}$ level is the ground state in ^{149}Ho (Ref. 16), ^{151}Ho (Ref. 13), ^{153}Ho (Ref. 17), ^{147}Tm (Ref. 18), and ^{153}Tm (Ref. 19). The indication from these energy systematics is that the $s_{1/2}$ orbital becomes a hole state at $Z=67$. Since the $s_{1/2}$ level is at ~ 67 keV in ^{147}Tm and at ~ 43 keV in ^{153}Tm, we estimate that its excitation energy in ^{151}Tm is ~ 50 keV.

As in Ref. 1 we compare (Fig. 6) experimental energy systematics for the five single-proton states in $N=82$ isotones with the results of spherical HFB calculations. Once again, hole states are plotted as having negative energies. In addition to the new ^{151}Tm results we have also updated the level information for ^{147}Tb and ^{149}Ho by using the data reported in Refs. 13 and 16, respectively. One notes in Fig. 6(a) the relatively smooth behavior of the proton orbitals from ^{133}Sb to ^{151}Tm. We therefore conclude as we did in Ref. 1, that these systematics indicate a modest gap at the $Z=64$ subclosure rather than a pronounced one as had been proposed by Nagai *et al.*[20] on the basis of their analysis of the same $N=82$ isotones. The calculated level energies, shown in Fig. 6(b), reproduce the experimental trends. In particular, the calculations for ^{151}Tm predict that the $s_{1/2}$ orbital is a hole state while the $h_{11/2}$ orbital represents the ground state. However, as pointed out in Ref. 1, the calculated excitation energies are too large, probably because the effective interaction is too strong.

We conclude this section by noting that direct evidence for ^{151}Yb^m *via* the $M4 \rightarrow M1$, $h_{11/2} \rightarrow d_{3/2} \rightarrow s_{1/2}$, cascade was not observed. The nonobservation of these two γ rays is consistent with both our low production for ^{151}Yb and our estimate of 4×10^{-3} for the isomeric decay branch. We estimated this branch based on systematics[1] of Weisskopf enhancements for the $M4$ transitions (1.8) in other even-Z $N=81$ isotones and on our measured 1.6-s half-life.

C. Levels in $^{151}_{68}Er_{83}$ from the decay of $^{151}_{69}Tm_{82}$

At the time that the present investigation was begun, only one transition, 801.6 keV, had been reported[21] to follow ^{151}Tm decay with a half-life of 3.8±0.8 s. During the preparation of this manuscript (our preliminary results were discussed in Ref. 22) work done by Barden *et al.*,[8] has appeared in print. They present a partial scheme with ten γ-ray transitions for the decay of ^{151}Tm which is in agreement with the more complete one that we have constructed. We do, however, disagree on some of the spin assignments.

We assigned a total of 86 γ rays to the decays of the $h_{11/2}$ ground and the $s_{1/2}$ isomeric ^{151}Tm states; energies and photon intensities for these transitions are listed in Tables II and III, respectively. Many of the γ rays can be seen in the singles spectra (Figs. 1 and 2) and in Fig. 3(b) where spectrum in coincidence primarily with Er $K\alpha_1$ x rays is shown. Based on the decay curves of several strong γ rays we deduce a half-life of 4.3±0.2 s for the $\frac{11}{2}^-$ ^{151}Tm ground state. This agrees with previously published values.[8,21] From the decay curve mea-

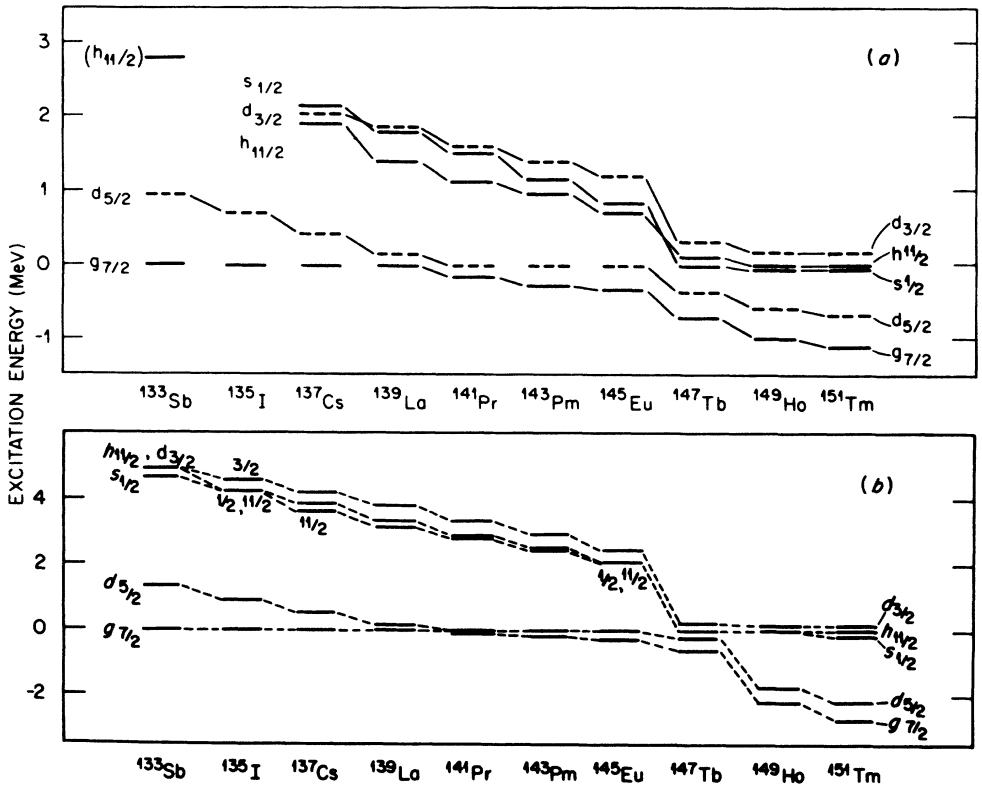

FIG. 6. Experimental [part (a)] and calculated [part (b)] energy systematics of single-proton states in odd-Z $N=82$ isotones. Note that hole states are plotted with negative energies.

sured for the 984.1-keV transition (see Table III) we determine a half-life of 8±2 s for the $s_{1/2}$ ^{151}Tm isomer; Barden *et al.*[8] report a half-life of 5.2±2.0 s.

Our proposed decay schemes (see Figs. 7 and 8) are based on $\gamma\gamma$-coincidence data, photon intensities, and, in a few cases, on γ-ray energy fits. Observed coincidences are indicated on the decay schemes. Absolute γ-ray intensities for 4.3-s and 8-s ^{151}Tm decays are obtained by requiring the sum of photon transition intensities to the ^{151}Er ground state to be 100% for each decay scheme. A Q_{EC} value of 7500 keV (Ref. 12) was used to compute logft values[23] for the (β^++EC) branches shown on the level schemes.

The ^{151}Er ground state has one neutron in the $f_{7/2}$ state above the $N=82$ closure, and the $i_{13/2}$, $h_{9/2}$, $p_{3/2}$, $p_{1/2}$, and $f_{5/2}$ states are vacant. The experimental energy systematics of these orbits for $N=83$ nuclei is shown in Fig. 9. A large part of the (β^++EC) strength from 4.3-s ^{151}Tm with its $\frac{11}{2}^-$ $(4\pi h_{11/2})_{J=0}$ $(\pi h_{11/2})$ configuration is expected to proceed *via* a $\pi h_{11/2} \rightarrow \nu h_{9/2}$ transition. The proton and neutron states involved in other (β^++EC) transitions are similar to those discussed in Sec. II B.

The low logft value for the β transition from the ^{151}Tm $h_{11/2}$ ground state to the 801.5-keV ^{151}Er level is consistent with the 801.5-keV level's $h_{9/2}$ assignment.[21] The 1140.2-keV state has also been seen[8,24] in the decay of a 0.6-s ^{151}Er isomer at 2586 keV and has been identified[8] as the $i_{13/2}$ single-particle state mixed with the $(\nu f_{7/2} \times 3^-)$ octupole vibration. From the energies of $\frac{13}{2}^+$ states in $N=83$ nuclei and of 3^- states in $N=82$ nuclei, an octupole admixture of $\simeq$45% was estimated. The energy pattern of 3^- states can also be considered in terms of the 3^- octupole states' microscopic structure where the largest component is $(\pi h_{11/2}\, \pi d_{5/2})$.

The transition strengths for the 1140.2-keV and 338.2-keV photons, by using the measured[24] half life of 10±3 ns and our measured branchings are $B(E3)=35\pm12$ W.u. and $B(M2)=0.45\pm0.10$ W.u., respectively. From the $M2$ retardation factor for the 338-keV γ ray, about 5 to 25% of the $\frac{9}{2}^-$ state was also deduced[8] to be admixed with the $(\nu f_{7/2} \times 2^+)$ collective excitation. The low logft values of 5.6±0.2 and 4.6±0.2 to the $\frac{13}{2}^+$ and $\frac{9}{2}^-$ levels, respectively, in the present work do not provide any conclusive information for the amount of collective-state admixtures.

Transitions from the 1496.0- and 1548.5-keV levels to the $\frac{7}{2}^-$ and $\frac{13}{2}^+$ states, combined with the logft values for the (β^++EC) decays, allow only $J^\pi=\frac{11}{2}^-$ and [considering uncertainties in (β^++EC) feedings] $\frac{9}{2}^+$ assignments for these levels. Barden *et al.*[8] proposed that the 1549-keV level is the best candidate, among the three levels at 1496, 1511, and 1549 keV, for being the $J^\pi=\frac{9}{2}^-, (\nu f_{7/2} \times 2^+)$ mixed significantly with the $\nu h_{9/2}$state. They did not, however, observe the 408.3-

TABLE II. Energies and photon intensities of transitions assigned to the decay of the $j_{11/2}$ state in ^{151}Tm.

E_γ(keV)	Level energy (keV)	I_γ (relative)[a]	I_γ (relative)[b] (Ref. 8)
136.9(4)	2212.7(7)	0.244(30)	
214.5(4)[c]		0.117(41)	
219.9(4)[c]		0.076(8)	
224.9(4)	1720.8(5)	0.42(9)	
241.3(6)[c]		0.17(4)	
272.9(6)[c]		0.33(7)	
332.7(6)[c]		0.57(12)	
338.3(6)	1140.2(3)	0.29(9)	
353.5(6)	2075.3(5)	0.44(11)	
354.2(6)	1495.8(4)	0.42(13)	
380.0(3)[c]		0.79(8)	
408.3(3)	1548.5(3)	0.57(6)	
417.1(3)[c]		0.57(6)	
446.7(4)[c]		0.54(5)	
478.6(6)[c]		1.07(21)	
526.7(4)	2075.3(5)	2.23(12)	
580.6(3)	1720.8(5)	2.70(27)	
677.6(4)[c]		0.24(5)	
692.8(7)	1495.8(4)	0.66(6)	
718.0(4)	2212.7(7)	0.67(7)	
765.8(4)	2449.5(6)	0.75(4)	
801.5(3)	801.5(3)	100(5)	100
818.6(10)	3031.1(5)	0.58(9)	
850.1(7)	3766.7(9)	0.69(23)	
865.5(7)[c]		0.49(5)	
893.5(6)[c]		0.41(4)	
919.3(4)	1720.8(5)	0.45(9)	
929.1(4)[c]		0.22(5)	
935.1(7)	2075.3(5)	0.40(8)	
956.1(7)	3031.1(5)	0.27(5)	
962.4(7)[c]		0.42(9)	
1071.3(10)	2212.7(7)	0.32(6)	
1092.7(4)	2776.2(6)	0.63(10)	
1097.4(6)[c]		0.79(24)	
1123.2(4)	3288.3(6)	1.33(7)	
1140.2(3)	1140.2(3)	15.6(8)	14
1199.0(10)	2921.6(6)	0.32(16)	
1326.2(5)	2874.7(6)	1.64(16)	
1363.6(3)	2165.1(5)	4.98(25)	4
1368.0(4)	2916.6(4)	0.94(9)	
1372.9(4)	2174.4(5)	1.22(12)	
1411.4(7)	2212.7(7)	0.57(9)	
1455.5(5)[c]		0.84(13)	
1483.0(7)	3031.1(5)	0.84(21)	
1488.5(4)	3037.3(5)	1.52(38)	
1495.8(4)	1495.8(4)	7.3(7)	7
1511.5(3)	1511.5(3)	2.8(8)	4
1525.9(4)	3037.3(5)	1.84(40)	
1535.6(3)	3031.1(5)	2.27(45)	
1548.5(3)	1548.5(3)	13.2(13)	14
1549.6(9)	3270.5(10)	1.52(16)	
1586.5(6)	3270.5(10)	0.55(27)	
1635.5(8)	2776.2(6)	0.70(35)	
1683.5(4)	1683.5(4)	1.85(19)	
1685.7(6)[c]		0.83(17)	
1761.7(7)[c]		0.80(8)	
1764.2(4)[c]		2.43(15)	
1777.1(10)	2916.6(4)	1.0(3)	

TABLE II. (*Continued*).

E_γ(keV)	Level energy (keV)	I_γ (relative)[a]	I_γ (relative)[b] (Ref. 8)
1809.8(3)	2611.3(5)	4.2(6)	4
1890.8(3)	3031.1(5)	3.19(23)	
1953.7(7)	3093.9(8)	0.41(6)	
2071.7(7)	3212.6(8)	0.98(40)	
2073.3(6)	2874.7(6)	1.11(45)	
2115.1(3)	2916.6(4)	16.9(9)	18
2120.1(4)	2921.6(6)	2.29(14)	
2140.2(7)[c]		0.41(12)	
2199.6(7)[c]		0.80(8)	
2229.7(4)	3031.1(5)	4.4(7)	4
2236.0(4)	3037.3(5)	2.54(40)	
2244.8(7)[c]		0.64(16)	
2313.6(10)	2313.6(10)	1.79(27)	
2329.6(10)	2329.6(10)	1.55(24)	
2411.9(10)	3212.6(8)	0.44(14)	
2449.5(6)	2449.5(6)	1.79(18)	
2451.1(6)	2451.1(6)	0.70(7)	
2469.7(9)	3270.5(10)	0.32(4)	
2539.2(25)	3340.7(30)	0.87(18)	
2921.7(25)	2921.6(6)	1.01(25)	
3037.5(25)	3037.3(5)	1.56(30)	
3110(3)	3110(3)	0.81(6)	

[a]Photon intensities are normalized to 100 for the 801.5-keV γ ray. For absolute intensities (which are shown on the level scheme in Fig. 7) multiply by (0.658±0.033). Conversion coefficients used to calculate total transition intensities ($I_\gamma + I_{ce}$) for some of the γ rays are as follows: $\alpha(136.9\gamma; M1/E2) = 1.06(13)$; $\alpha(224.9\gamma; M1/E2) = 0.23(6)$; $\alpha(338.3\gamma; M2) = 0.380$; $\alpha(353.5\gamma; M1/E2) = 0.065(23)$; $\alpha(354.2\gamma; E2) = 0.0424$, $\alpha(408.3\gamma; E2) = 0.0283$; $\alpha(526.78; M1/E2) = 0.023(8)$; $\alpha(580.6\gamma; M1/E2) = 0.018(7)$; and $\alpha(801.5\gamma; M1) = 0.0109$.

[b]Normalized to 100 at the 801.5-keV γ ray.

[c]Not placed in level scheme. Some of the γ rays above 1 MeV in energy may belong to the decay of the $s_{1/2}$ state in ^{151}Tm (γ rays below 1 MeV are seen in coincidences with some of the strong γ rays of $11/2^-$ ^{151}Tm decay).

keV γ-ray transition to the $\frac{13}{2}^+$ level which makes the $\frac{9}{2}^-$ assignment unlikely.

The first 2^+ collective state in ^{150}Er is at 1578.9 keV.[25] The $\frac{11}{2}^-, \frac{9}{2}^-, \ldots$ states of the $(\nu f_{7/2} \times 2^+)$ particle-core coupling in ^{151}Er are expected to be close to this energy (see, e.g., Ref. 26). The 1511.5-keV level in ^{151}Er could possibly be the $\frac{9}{2}^-$, or $\frac{11}{2}^-$ member. This level decays only to the ground state, and it is fed very weakly, if at

TABLE III. Energies and photon intensities of transitions assigned to the decay of the $s_{1/2}$ state in ^{151}Tm.

E_γ (keV)	Level energy (keV)	I_γ (relative)[a]	I_γ (relative)[b]
222.1(4)	1206.2(6)	2.9(6)	0.116(24)
984.1(4)	984.1(4)	100(20)	4.0(8)
1048.3?(6)	2032.4(8)	2.6(9)	0.103(36)
1637.4(5)	2621.5(7)	33(7)	1.31(27)
1982(2)	2966(2)	16(7)	0.64(29)
2067(2)	3051(2)	16(7)	9.64(26)

[a]Relative photon intensities are normalized to $I(984.1\gamma) = 100$ per 100 decays of the $s_{1/2}$ state in ^{151}Tm. This absolute normalization could be an upper limit if there are more transitions decaying directly to the ^{151}Er ground state. A conversion coefficient of $\alpha(M1) = 0.307$ was used for calculating the total intensity shown in the level scheme for the 222.1-keV transition.

[b]Relative photon intensities normalized to a value of 100 for the 801.5-keV transition (see Table II) that follows the decay of the $h_{11/2}$ state in ^{151}Tm.

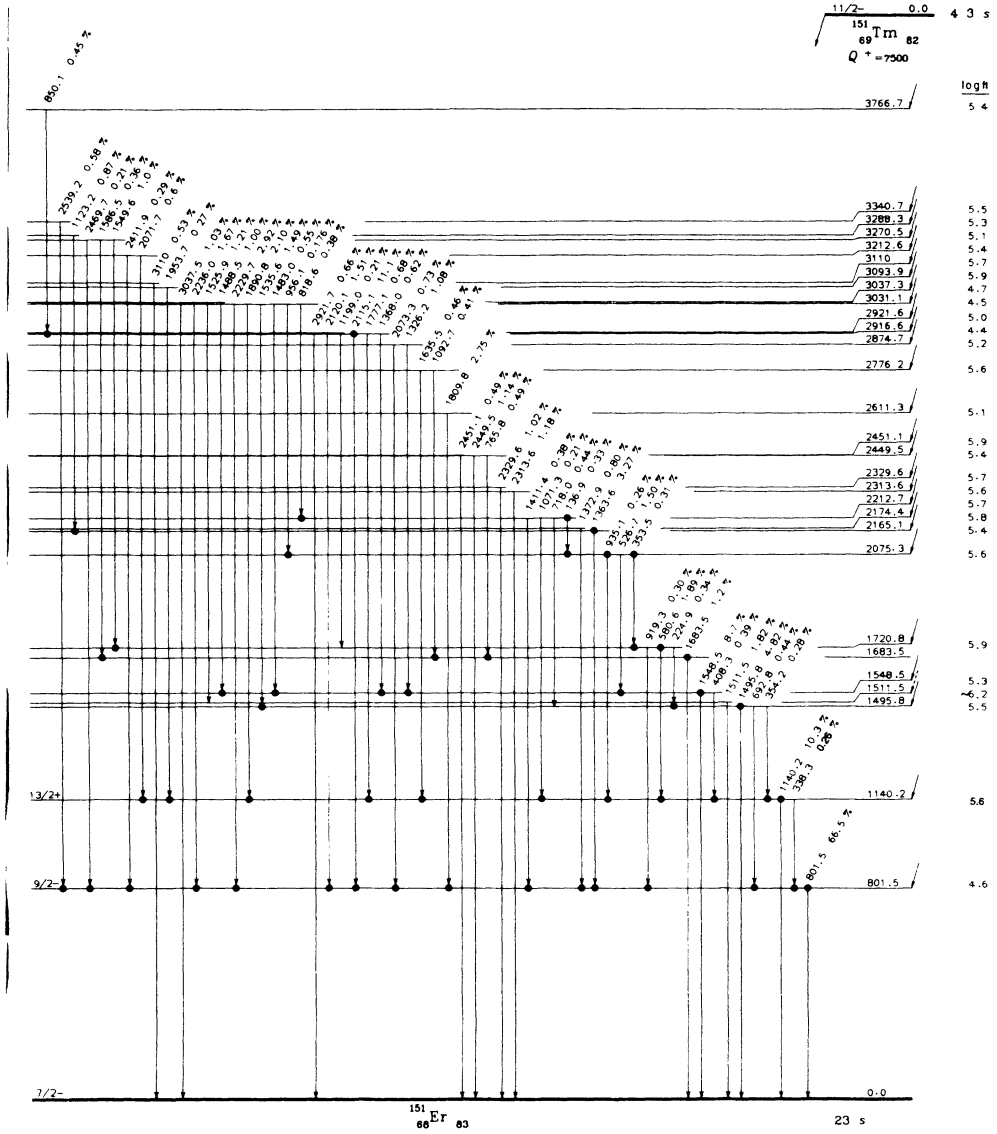

FIG. 7. Proposed decay scheme for the $h_{11/2}$ ground state of ^{151}Tm. Total intensities per 100 decays of the parent state are given following the γ-ray energies. Observed coincidences are indicated in the figure by dots in the conventional manner.

all, by the $(\beta^+ + \text{EC})$ decay of $h_{11/2}$ ^{151}Tm.

The $(\beta^+ + \text{EC})$ transitions to the 2916.6-, 3031.1-, and 3037.2-keV levels have low logft values of 4.4, 4.5, and 4.7, respectively, if one assumes that there is no appreciable feeding from higher excitation energies by some of the unplaced γ rays listed in Table II or by high-energy γ rays outside of our detection range. These allowed $(\beta^+ + \text{EC})$ transitions determine the parities of the three levels to be negative and the spins to be $\frac{9}{2}$, $\frac{11}{2}$, or $\frac{13}{2}$. By considering the available proton and neutron states, one infers that these fast $(\beta^+ + \text{EC})$ transitions most probably involve the $\pi h_{11/2} \rightarrow \nu h_{9/2}$ transition. The 3037.2-keV level deexcites by equally strong γ rays to the $\nu f_{7/2}$ and $\nu h_{9/2}$ states. Because of γ rays proceeding to the $\frac{9}{2}^-$ and $\frac{13}{2}^+$ states, the spins ($\pi = -$ from logft value) of the 2916.6- and 3031.1-keV levels must be $\frac{11}{2}^-$ or $\frac{13}{2}^-$. Intensities of the deexciting γ rays suggest that the characters for these two levels are not the same.

The 2916.6- and 3031.1-keV levels were also observed by Barden *et al.*[8] who suggested $[(\pi h_{11/2}, \nu h_{9/2})_{J=1} + \pi h_{11/2}]$ $\frac{9}{2}^-$, $\frac{11}{2}^-$, $\frac{13}{2}^-$ configurations for them, populated through a proton of an $h_{11/2}$ pair in ^{151}Tm decaying to the $\nu h_{9/2}$ state. Spin of $\frac{9}{2}^-$ is unlikely from their decays to the $\frac{13}{2}^+$ level, and the proposed composition is inconsistent with the levels' decay patterns. The 2229.7- and 1890.8-keV γ rays from the 3031.1-keV level, for example, populate the $\frac{9}{2}^-$ and $\frac{13}{2}^+$ states with about equal intensity which would require a $\nu h_{9/2} \rightarrow \nu i_{13/2}$ γ transition to compete with the transition to the $\nu h_{9/2}$ state.

The $\frac{1}{2}^+$ isomer in ^{151}Tm was produced through ^{151}Yb

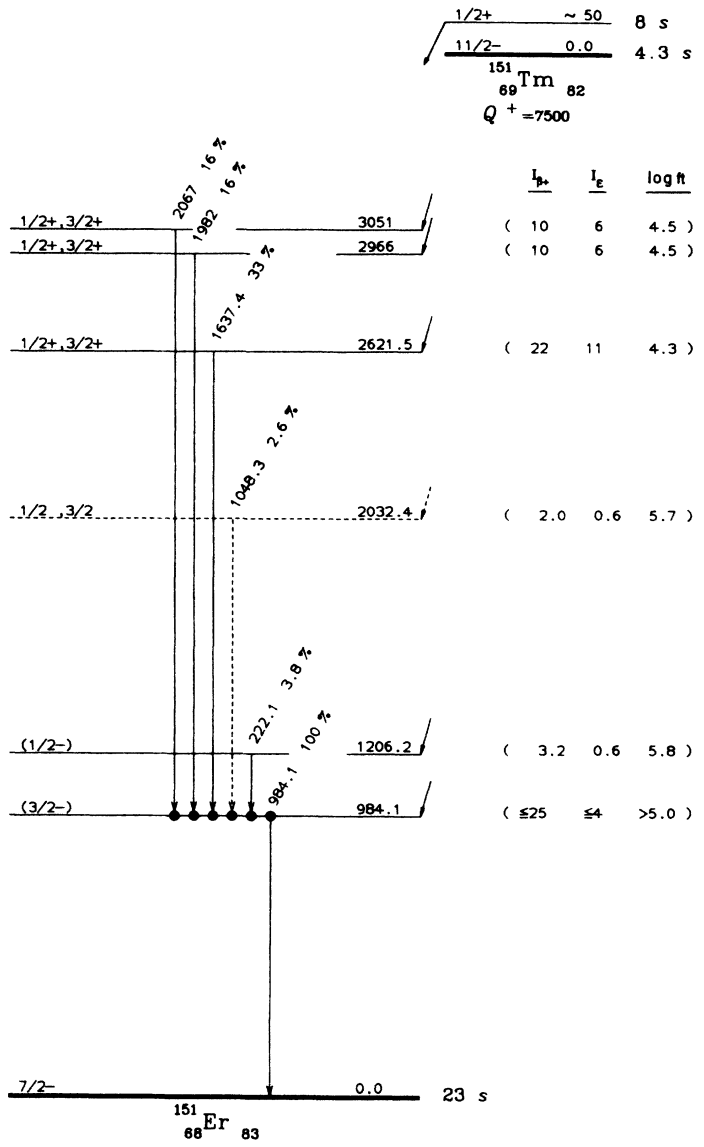

FIG. 8. Proposed decay scheme for the $s_{1/2}$ isomer in ^{151}Tm. Total intensities per 100 decays of parent level are given following the γ-ray energies. Observed coincidences are indicated by dots in the conventional manner.

decay and through (3p2n) evaporation from the compound system. Its total production is calculated from the intensities of the 801.5- and 984.1-keV γ rays to be about 2.6% of that for the $\frac{11}{2}^-$ ^{151}Tm ground state. Because of this low yield, only a few γ rays could be assigned to 8-s ^{151}Tm and their identification is based on coincidences with the 984.1-keV γ ray.

The spin and parities of levels shown in Fig. 8 above 2-MeV excitation are deduced from logft values. Since the level at 984.1 keV is populated by a (β^+ + EC) branch from the $\frac{1}{2}^+$ state and it decays to the $\frac{7}{2}^+$ ground state, we assign the $\nu p_{3/2}$ shell state to this level in analogy to the $p_{3/2}$ states in $N=83$ nuclei with $Z<68$. The same assignment was made in Ref. 8.

The $p_{1/2}$ state is also expected to be populated in 8-s ^{151}Tm decay *via* $\pi s_{1/2} \rightarrow \nu p_{1/2}$ transition. The experimental energies of the $\frac{1}{2}^-$ neutron states follow a trend similar to the $p_{3/2}$ states spectrum (see Fig. 9). In the β decay of $\frac{1}{2}^-$ ^{149}Ho [$T_{1/2}=54$ s (Ref. 27)] levels have been observed[28] in ^{149}Dy at 1407.2 keV and eight more at higher energies above the $\frac{3}{2}^-$ state at 1034.9 keV. The levels above 2 MeV have positive parities based on logft values for their β feedings. The 1407.2-keV level is the most probable candidate for the $\nu p_{1/2}$ state in ^{149}Dy. In ^{151}Er, among the β^- transitions to levels above the $p_{3/2}$ state (see Fig. 8), only the β^- decays to the 1206.2- and 2032.4-keV levels could be first forbidden. Therefore, these levels may be candidates for the $\frac{1}{2}^-$ state. The 1206.2-keV level in ^{151}Er fits the $\frac{1}{2}^-$ energy systematics rather smoothly (see Fig. 9); the level at 2032.3 keV does not. We therefore, tentatively, propose a $\nu p_{1/2}$ configuration for the 1206.2-keV level.

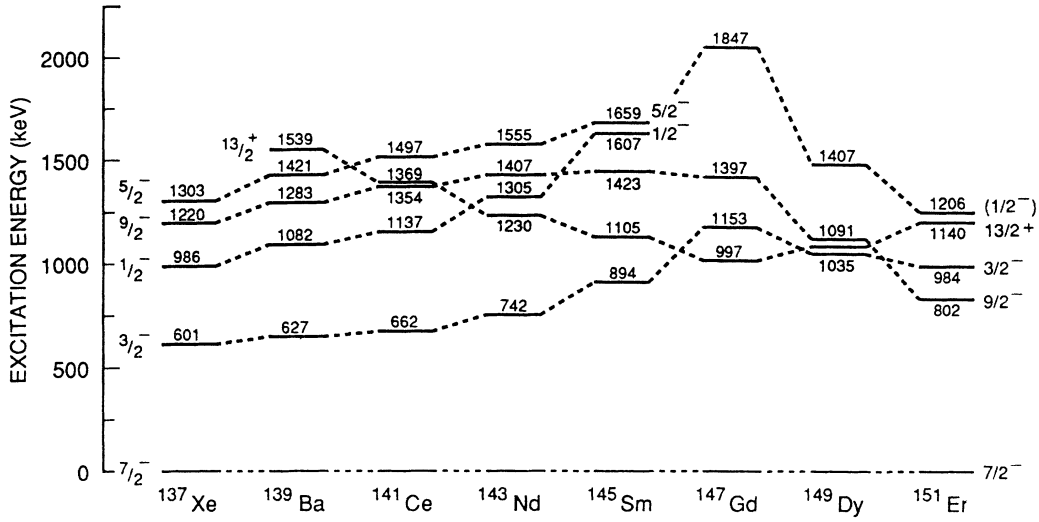

FIG. 9. Experimental energy systematics of lowest states in even-Z $N=83$ isotones. Level energies for ^{137}Xe through ^{147}Gd are taken from the Nuclear Data Sheets; for ^{149}Dy from Ref. 28; for ^{151}Er from this work.

III. HARTREE-FOCK-BOGOLIUBOV (HFB) CALCULATIONS

The spectra of the $N=83$ nuclei are calculated with the spherical HFB theory. The model space is given in Ref. 29. Since the valence space does not permit radial mixing, the HFB equations separate into coupled Hartree-Fock (HF) and Bardeen-Cooper-Schrieffer (BCS) equations

$$\epsilon_{j\tau}=e_{j\tau}+\Gamma_{j\tau} , \tag{1}$$

$$\Gamma_{j\tau}=\sum_{j'\tau'} V_{j\tau,j'\tau'}(2j'+1)v^2_{j'\tau'} , \tag{2}$$

$$V_{j\tau,j'\tau'}=(2j+1)^{-1}(2j'+1)^{-1}\sum_J (2J+1)\langle j\tau j'\tau' J|v_a|j\tau j'\tau' J\rangle , \tag{3}$$

$$\Delta_{j\tau}=\tfrac{1}{2}(2j+1)^{-1/2}\sum_{j'}(-1)^{l+l'}(2j'+1)^{1/2}\langle j^2 J=0\ T=1|v_a|(j')^2 J=0\ T=1\rangle u_{j'\tau}v_{j'\tau} , \tag{4}$$

where e is the inert core energy, ϵ is the HF single-particle energy, Γ is the HF potential, Δ is the pair potential, and τ is π (proton) or ν (neutron). The energy contribution to $\Gamma_{j\tau}$ due to one nucleon in the orbit $j'\tau'$ is $V_{j\tau,j'\tau'}$. The relevant matrix elements of V are given in Table IV. The orbital occupation probability is

$$v^2_{j\tau}=\tfrac{1}{2}[1-(\epsilon_{j\tau}-\lambda_\tau)/E_{j\tau}] , \tag{5}$$

where the quasiparticle energies are

$$E_{j\tau}=[(\epsilon_{j\tau}-\lambda_\tau)^2+\Delta^2_{j\tau}]^{1/2} , \tag{6}$$

and $u^2+v^2=1$. The $N=83$ nucleus is described as a one quasineutron excitation of the $N=82$ core. The excitation energies of the $N=83$ nucleus are

$$E'_{j\nu}=E_{j\nu}-E_{o\nu} , \tag{7}$$

where $E_{o\nu}$ is the smallest quasineutron energy.

The inert core energies are chosen so that the HFB single-particle energies agree with the experimentally deduced[30] single-particle energies in ^{146}Gd. The interaction is the Brueckner G matrix derived from the Reid soft-core potential.[31] This interaction is used to calculate the pairing gaps as well as the single-particle energies.

The calculated $N=83$ spectra are shown in Fig. 10.

TABLE IV. Matrix elements $V_{j\nu,j'\pi}$.[a]

$j\nu$ \ $j'\pi$	$3s_{1/2}$	$2d_{3/2}$	$2d_{5/2}$	$1g_{7/2}$	$1h_{11/2}$
$3p_{1/2}$	−0.675	−0.464	−0.559	−0.302	−0.282
$3p_{3/2}$	−0.790	−0.511	−0.492	−0.312	−0.270
$2f_{5/2}$	−0.494	−0.458	−0.568	−0.356	−0.349
$2f_{7/2}$	−0.479	−0.609	−0.495	−0.388	−0.309
$1h_{9/2}$	−0.350	−0.372	−0.414	−0.470	−0.596
$1i_{13/2}$	−0.303	−0.358	−0.316	−0.514	−0.372

[a] $V_{j\nu,j'\pi}$ is the contribution to the neutron spherical HF potential $\Gamma_{j\nu}$ due to one proton in the subshell j'. See Eq. (3). These are for the unscaled interaction.

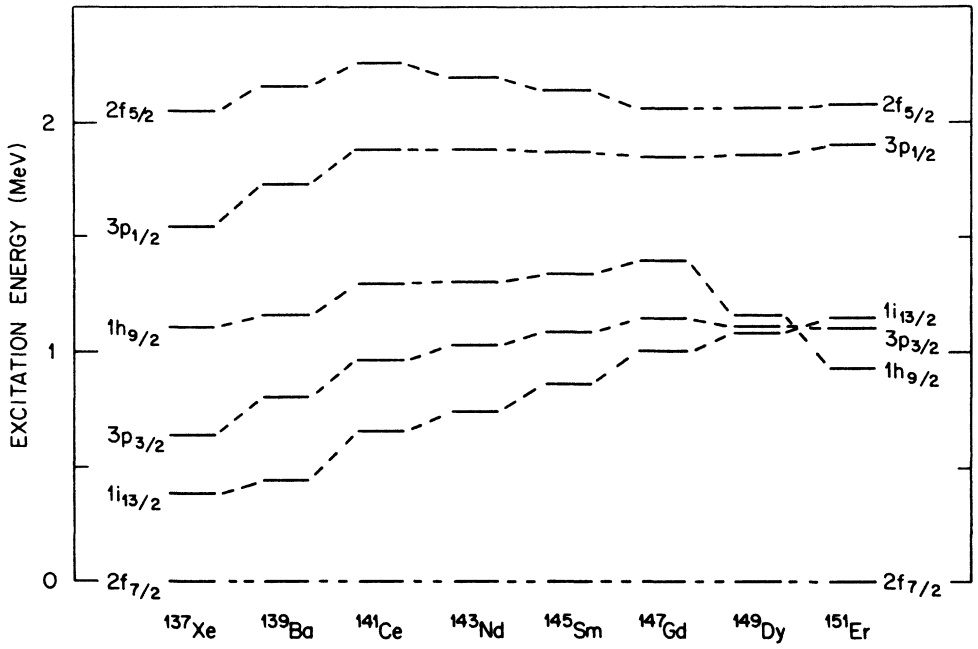

FIG. 10. Energy systematics of HFB single-neutron states in $N=83$ even-Z nuclei. The interaction is not scaled (see text).

Comparing with the experimental spectra in Fig. 9, it is apparent that the systematics are not reproduced. Most notably, the experimental $\frac{13}{2}^+$ level decreases with Z from ^{137}Xe to ^{147}Gd, whereas the calculated $1i_{13/2}$ level increases with Z. Comparing the calculated and experimental spectra for ^{137}Xe, one sees that the calculated $3p_{1/2}$, $2f_{5/2}$, and $1i_{13/2}$ levels have the wrong energy.

Why does the spherical HFB calculation fail to reproduce the experimental energy systematics? There are two possible reasons. First, the spherical HFB theory only includes single-particle excitations. If a particular experimental level contains a significant component which is collective and not single-particle in nature, then one should not expect the spherical HFB theory to give a correct description of that particular energy level. This may be the reason why Fig. 10 gives the wrong systematics for the $\frac{13}{2}^+$ levels (see Sec. II C).

There is a second reason why the spherical HFB calculation might fail to reproduce experimental energy systematics. Perhaps the interaction used may not be the correct effective interaction for these nuclei. If the correct interaction were used, then perhaps the energy systematics would be reproduced. We will take this possibility seriously and adopt the point of view often expressed by Talmi.[32] The experimental spectrum of one nucleus may be used to infer a set of effective interaction matrix elements. These matrix elements can then be used to calculate the spectra of other nuclei. We follow this procedure for the $N=83$ spectra. For purposes of illustration, we leave the $i_{13/2}$ level in the calculation. However, we emphasize that we do not claim that the experimental $\frac{13}{2}^+$ states can be described as $\nu i_{13/2}$.

To identify the relevant matrix elements, consider how the $3p_{3/2}$ neutron level varies with increasing Z. For nuclei between ^{137}Xe and ^{147}Gd, protons are being added to the $2d_{5/2}$ and $1g_{7/2}$ orbitals. The interaction between the $3p_{3/2}$ neutron and a proton in the $2d_{5/2}$ and $1g_{7/2}$ orbitals determines how the $3p_{3/2}$ level varies with Z. Similarly, for nuclei heavier than ^{147}Gd ($Z>64$), protons are added to the $3s_{1/2}$, $2d_{3/2}$, and $1h_{11/2}$ orbitals. The interaction between the $p_{3/2}$ neutron and those proton orbitals determines how the $3p_{3/2}$ level varies with Z for $Z>64$. Similar arguments apply for the other neutron energy levels.

This argument can be put into a quantitative form by calculating the variation of an $N=83$ excitation energy with proton number

$$\frac{dE'_{j\nu}}{dZ}=\frac{d}{dZ}(E_{j\nu}-E_{o\nu}) . \tag{8}$$

If $\Delta_{j\nu}$ and $\Delta_{o\nu}$ are zero, then

$$\frac{dE'_{j\nu}}{dZ}=\frac{d}{dZ}(\epsilon_{j\nu}-\epsilon_{o\nu}) = \sum_{j'\tau'}[V_{j\nu,j'\tau'}-V_{o\nu,j'\tau'}](2j'+1)\frac{d}{dZ}v^2_{j'\tau'} . \tag{9}$$

If Δ is not zero, but is approximately constant with Z, then the first equality in Eq. (9) becomes an approximation. Equation (9) shows that the variation with Z of a particular neutron excitation energy is determined by those orbits which have a nonzero value of dv^2/dZ. These are primarily the proton orbits which are being filled, such as the $2d_{5/2}$ and $1g_{7/2}$ orbits for nuclei between ^{137}Xe and ^{147}Gd, and the $3s_{1/2}$, $2d_{3/2}$, and $1h_{11/2}$ orbits for nuclei heavier than ^{147}Gd. Consequently, for nuclei between ^{137}Xe and ^{147}Gd, the variation of the $3p_{3/2}$

TABLE V. Scale factor $\chi_{j\nu,j'\pi}$.[a]

jv \ $j'\pi$	$2d_{5/2}$ $1g_{7/2}$	$3s_{1/2}$ $2d_{3/2}$ $1h_{11/2}$
$3p_{1/2}$	0.85	1.50
$3p_{3/2}$	0.97	1.08
$2f_{5/2}$	0.80	1.00
$2f_{7/2}$	1.00	1.00
$1h_{9/2}$	0.98	1.05
$1i_{13/2}$	1.33	1.03

[a]The factor χ scales the effective interaction. See Eq. (10).

excitation energy can be altered simply by changing the values of $V_{p_{3/2}\nu,d_{5/2}\pi}$ and $V_{p_{3/2}\nu,g_{7/2}\pi}$.

A phenomenological scale factor χ is introduced to define new effective interaction matrix elements

$$V'_{j\nu,j'\pi}=\chi_{j\nu,j'\pi}V_{j\nu,j'\pi}\ . \tag{10}$$

We reduce the number of free parameters in χ by using the same value of χ for $j'=2d_{5/2}$, $1g_{7/2}$ and the same χ for $j'=3s_{1/2}$, $2d_{3/2}$, $1h_{11/2}$. The values of χ are chosen as follows: The experiment has $dE'_{p_{3/2}\nu}/dZ<0$ for nuclei from ^{147}Gd to ^{151}Er. The original interaction gives $dE'_{p_{3/2}\nu}/dZ\approx 0$. Since $dv^2_{s_{1/2}\pi}/dZ>0$, $dv^2_{d_{3/2}\pi}/dZ>0$, and $dv^2_{h_{11/2}\pi}/dZ>0$, Eq. (9) suggests that this discrepancy can be eliminated by increasing the attraction between the $3p_{3/2}$ neutron and the $3s_{1/2}$, $2d_{3/2}$, and $1h_{11/2}$ protons. Consequently the scale factor χ must be greater than unity for these matrix elements.

The value of $\chi_{p_{3/2}\nu,s_{1/2}\pi}(=\chi_{p_{3/2}\nu,d_{3/2}\pi}=\chi_{p_{3/2}\nu,h_{11/2}\pi})$ is varied until the calculated and experimental $\frac{3}{2}^-$ excitation energies agree in ^{151}Er. At the same time the core energy $e_{p_{3/2}\nu}$ is varied so that the calculated and experimental $\frac{3}{2}^-$ energies remain in agreement for ^{147}Gd. Next $\chi_{p_{3/2}\nu,d_{5/2}\pi}(=\chi_{p_{3/2}\nu,g_{7/2}\pi})$ is varied until the calculated and experimental $\frac{3}{2}^-$ energies agree in ^{137}Xe. The new set of matrix elements $V'_{p_{3/2}\nu,j'\pi}$ is now determined.

This procedure is repeated for other neutron orbitals: $3p_{1/2}$, $2f_{5/2}$, $1h_{9/2}$, and $1i_{13/2}$. The interaction of the $2f_{7/2}$ neutron ground state with the protons is not scaled. Since the experimental $\frac{5}{2}^-$ level has not been identified in ^{149}Dy or ^{151}Er, the matrix element $V_{f_{5/2}\nu,s_{1/2}\pi}$ is not scaled. The values of χ are given in Table V. The new set of matrix elements $V'_{j\nu,j'\pi}$ and core energies $e_{j\nu}$ is now completely determined.

The spectral of the $N=83$ nuclei obtained with this new effective interaction are given in Fig. 11. It should be emphasized that the *same* matrix elements and core energies are used for *all* nuclei. It should also be emphasized that the number of free parameters introduced by scaling the interaction is small compared to the number of calculated levels. From Table V observe that only nine scale factors differ from unity. These are the parameters. Also five of these nine parameters are very close to unity. Setting them equal to 1 would only produce small changes in the spectra. So only four parameters are required to calculate spectra similar to Fig. 11. The number of calculated level energies is 35. The levels of ^{147}Gd are not included in this number, since this nucleus is fit by the choice of core energies.

Compare the systematics of the experimental spectra in Fig. 9 and the new calculations in Fig. 11. The agree-

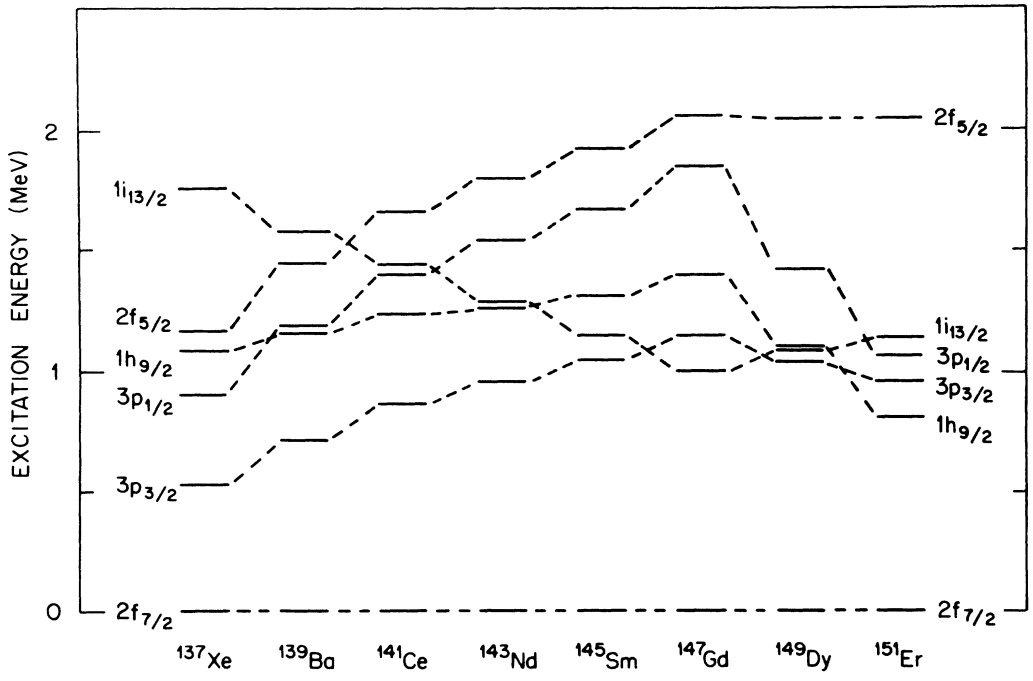

FIG. 11. Energy systematics of HFB single-neutron states in $N=83$ even-Z nuclei. The interaction is scaled by χ (see text).

ment is dramatically improved. The calculated systematics are now in excellent agreement with experiment.

Finally, it should be noted that the HFB spectra in Fig. 11 could be improved even further. The scale factors χ were not determined by a least squares fit to the data, but rather by two or three iterated guesses. Also, one could relax the requirement that the same values of χ be used for the $2d_{5/2}$ and $1g_{7/2}$ proton orbits, and for the $3s_{1/2}$, $2d_{3/2}$, and $1h_{11/2}$ proton orbits. This, however, would increase the number of parameters.

We have shown that the experimental spectra can be used to scale a few selected matrix elements, thereby defining a new effective interaction. Using this new interaction, the HFB spectra agree with the experimental systematics. The conclusion is that a single-particle description can provide the $N=83$ energy systematics, if the proper Hamiltonian is used.

We conclude with some comments regarding the $\frac{13}{2}^+$ states. It has been suggested that these states are a mixture of $\nu i_{13/2}$ and a 3^- octupole phonon coupled to $\nu f_{7/2}$ (see discussion in Sec. II C). One argument used to justify this assignment is that the $\frac{13}{2}^+$ states in $N=83$ isotones track the energies of the 3^- states in the corresponding $N=82$ nuclei, thereby explaining the $\frac{13}{2}^+$ energy systematics. What we have demonstrated is that this argument alone is not sufficient to demonstrate the octupole phonon admixture in the $\frac{13}{2}^+$ states. We have shown that a single-particle description can explain the energy systematics of the $\frac{13}{2}^+$ states, if the proper Hamiltonian is used. Therefore, the second argument based upon $B(E3)$ values become crucial for demonstrating the octupole phonon admixture. Once we admit this additional evidence, then the spherical HFB theory cannot properly describe the $\frac{13}{2}^+$ states. Furthermore, the scaled effective interaction for the $\nu i_{13/2}$ state becomes spurious, since it is derived, in part, from the incorrect assumption that the experimental $\frac{13}{2}^+$ energies can be identified as $\nu i_{13/2}$ energies.

ACKNOWLEDGMENTS

The authors would like to thank M. J. Martin for his critical review of this paper and for his helpful suggestions. Oak Ridge National Laboratory is operated by Martin Marietta Energy Systems, Inc. for the U.S. Department of Energy under Contract No. DE-AC05-840R21400. Research at the Tulane University Physics Department was supported in part by the National Science Foundation. Work at the Lawrence Berkeley Laboratory was supported by the U.S. Department of Energy under Contract No. DE-AC03-76SF00098.

[1]K. S. Toth, Y. A. Ellis-Akovali, F. T. Avignone III, R. S. Moore, D. M. Moltz, J. M. Nitschke, P. A. Wilmarth, P. K. Lemmertz, D. C. Sousa, and A. L. Goodman, Phys. Rev. C **32**, 342 (1985).

[2]J. D. Molitoris and J. M. Nitschke, Nucl. Instrum. Methods **186**, 659 (1981).

[3]J. M. Nitschke, Nucl. Instrum. Methods **206**, 341 (1983).

[4]K. S. Toth, D. C. Sousa, J. M. Nitschke, and P. A. Wilmarth, Phys. Rev. C **35**, 310 (1987).

[5]M. Blann and F. Plasil, U.S. Atomic Energy Commission Report No. C00-3594-10, 1973; also W. G. Winn, H. H. Gutbrod, and M. Blann, Nucl. Phys. **A188**, 423 (1972).

[6]K. S. Toth, R. L. Hahn, M. A. Ijaz, and W. M. Sample, Phys. Rev. C **2**, 1480 (1970).

[7]Y. A. Ellis-Akovali, K. S. Toth, D. M. Moltz, and J. D. Cole, in *Proceedings of the International Conference on Nuclear Structure, Amsterdam, 1982,* edited by A. van der Woude and B. J. Verhaar (North-Holland, Amsterdam, 1982), Vol. I, p. 64.

[8]R. Barden, A. Płochocki, D. Schardt, B. Rubio, M. Ogawa, P. Kleinheinz, R. Kirchner, O. Klepper, and J. Blomqvist, Z. Phys. A **329**, 11 (1988).

[9]K. S. Toth, D. M. Moltz, E. C. Schloemer, M. D. Cable, F. T. Avignone, III, and Y. A. Ellis-Akovali, in *Proceedings of the Seventh International Conference on Atomic Masses and Fundamental Constants, Darmstadt, 1984,* edited by O. Klepper (Technische Hochschule, Darmstadt, 1984), p. 237.

[10]K. S. Toth, Y. A. Ellis-Akovali, J. M. Nitschke, P. A. Wilmarth, P. K. Lemmertz, D. M. Moltz, and F. T. Avignone III, Phys. Lett. B **178**, 150 (1986).

[11]P. Kleinheinz, B. Rubio, M. Ogawa, M. Piiparinen, A. Płochocki, D. Schardt, R. Barden, O. Klepper, R. Kirchner, and E. Roeckl, Z. Phys. A **323**, 705 (1985).

[12]A. H. Wapstra and G. Audi, Nucl. Phys. **A432**, 1 (1985).

[13]C. F. Liang, P. Paris, P. Kleinheinz, B. Rubio, M. Piiparinen, D. Schardt, A. Płochocki, and R. Barden, Phys. Lett. B **191**, 245 (1987).

[14]D. J. Decman, L. G. Mann, G. L. Struble, D. H. Sisson, C. M. Henderson, H. J. Scheerer, P. Kleinheinz, K. E. Thomas, and H. A. O'Brien, in *Proceedings of the Seventh International Conference on Atomic Masses and Fundamental Constants, Darmstadt, 1984,* edited by O. Klepper (Technische Hochshule, Darmstadt, 1984), p. 220.

[15]B. A. Alikov, Ya. Vavryschchuk, K. Ya. Gromov, G. I. Lizurei, M. M. Malikov, T. M. Muminov, Sh. Omanov, and R. R. Usmanov, Ivz. Akad. Nauk SSSR, Ser. Fiz. **42**, 797 (1978).

[16]R. B. Firestone, J. M. Nitschke, P. A. Wilmarth, K. Vierinen, J. Gilat, K. S. Toth, and Y. A. Akovali, Lawrence Berkeley Laboratory Report No. LBL-24652, 1987.

[17]W.-D. Schmidt-Ott, K. S. Toth, E. Newman, and C. R. Bingham, Phys. Rev. C **10**, 296 (1974).

[18]S. Hoffman, Y. K. Agarwal, F. P. Hessberger, P. O. Larsson, G. Münzenberg, K. Poppensieker, J. R. H. Schneider, and H. J. Schött, *Proceedings of the Seventh International Conference on Atomic Masses and Fundamental Constants, Darmstadt, 1984,* edited by O. Klepper (Technische Hochschule, Darmstadt, 1984), p. 184.

[19]K. S. Toth, P. A. Wilmarth, J. M. Nitschke, K. Vierinen, M. O. Kortelahti, and F. T. Avignone III, Phys. Rev. C (to be published).

[20]Y. Nagai, J. Styczen, M. Piiparinen, P. Kleinheinz, D. Baz-

zacco, P. V. Brentano, K. O. Zell, and J. Blomqvist, Phys. Rev. Lett. **47**, 1259 (1981).

[21]E. Nolte, G. Korschinek, and Ch. Setzensack, Z. Phys. A **309**, 33 (1982).

[22]Y. A. Ellis-Akovali, M. N. Rao, K. S. Toth, A. L. Goodman, J. M. Nitschke, and P. A. Wilmarth, Bull. Am. Phys. Soc. **32**, 1018 (1987).

[23]N. B. Gove and M. J. Martin, Nucl. Data Tables **A10**, 205 (1971).

[24]J. Jastrzebski, R. Kossakowski, J. Lukasiak, M. Moszyński, Z. Preibisz, S. André, J. Genevey, A. Gizon, and J. Gizon, Phys. Lett. **97B**, 50 (1980).

[25]E. Nolte, S. Z. Gui, G. Colombo, G. Korschinek, and K. Eskola, Z. Phys. A **306**, 223 (1982).

[26]Z. Haratym, J. Kownacki, J. Ludziejewski, Z. Sujkowski, L.-E. De Geer, A. Kerek, and H. Ryde, Nucl. Phys. **A276**, 299 (1977).

[27]K. S. Toth, J. M. Nitschke, P. A. Wilmarth, Y. A. Ellis-Akovali, D. C. Sousa, K. Vierinen, D. M. Moltz, J. Gilat, and N. M. Rao, in *Nuclei Far from Stability (Ontario, 1987)*, Proceedings of the Fifth International Conference on Nuclei Far from Stability, AIP Conf. Proc. No. 164, edited by Ian S. Towner (AIP, New York, 1987), p. 178.

[28]R. B. Firestone, K. S. Toth, Y. A. Akovali, J. M. Nitschke, P. A. Wilmarth, K. Vierinen, and J. Gilat (unpublished).

[29]A. L. Goodman, Nucl. Phys. **A331**, 401 (1979).

[30]P. Kleinheinz, R. Broda, P. J. Daly, S. Lunardi, M. Ogawa, and J. Blomqvist, Z. Phys. A **290**, 279 (1979).

[31]A. L. Goodman, J. P. Vary, and P. A. Sorenson, Phys. Rev. C **13**, 1674 (1976).

[32]See, for example, Amos de-Shalit and Igal Talmi, *Nuclear Shell Theory* (Academic, New York, 1963).